Engineering Solid Mechanics 8 (2020) 245-252

Contents lists available at GrowingScience

Engineering Solid Mechanics

homepage: www.GrowingScience.com/esm

A creative rapid assembly modular free form pavement for post-disaster temporary roads and sidewalks

Yahya Aliabadizadeh[a], Farzaneh Tahmoorian[b], Saeed Nemati[c*], Bijan Samali[d] and Pezhman Sharafi[d]

[a]*University of Maryland, College Park, Maryland, USA*
[b]*School of Engineering and Technology, Central Queensland University, Australia*
[c]*World Civil Engineering Information Centre, Australia*
[d]*Centre for Infrastructure Engineering, Western Sydney University, Australia*

ARTICLEINFO

Article history:
Received 16 October 2019
Accepted 26 December 2019
Available online
26 December 2019

Keywords:
Post- Disaster
Temporary Roads
Polyurethane (PU) foam
Free form pavement

ABSTRACT

Immediate aid to survivors of a natural disaster is the keynote to crisis management. Providing temporary access is one of the most important principles of immediate relief. However, in the post-disaster conditions, it is not possible to use road construction machinery, especially in rural areas. Therefore, in this study, the feasibility of using a Rapid Assembly Building (RAB) system for the temporary pavement with the possibility of rapid construction, which follows the natural topography of the place, is investigated. The introduced system consists of a high-density polyurethane (PUR) foam core as well as two continuous layers of high-density polyethylene (HDPE) facings. For this purpose, the mechanical properties of the materials and composite pavement were determined by a series of laboratory tests. Then, the mechanical performance and bearing behaviour of an element of the presented pavement system was numerically modelled under AASHTO loading. Since in the post-disaster situation, it is not possible to establish the subgrade, an un-compacted subgrade is used for modelling. The results show that this system can be used well in post-disaster situations to provide a rapid, safe, yet robust road without any permanent deformation.

1. Introduction

Crisis management after natural disaster such as floods and earthquakes can be a severe concern of governments. In the event of crises, quick decision making is a fundamental component of a successful post-disaster management framework (Tsai, 2014; Dandan, 2007). Specialists appraise that usually it can take about 8 years for countries to recoup from the impacts of a natural or unnatural disaster, which highlights the seriousness of the catastrophe and the significance of RABs (Goodyear, 2014; Goodyear & Fabian 2014). On the other hand, temporary roads are important parts of the urban post-disaster traffic system. In this regard, rapidly assembled panels are used commonly in all post-disaster structures, but there is not any rapidly assembled pavement system yet (Development, 2014). Also, as the size of panelised components increments, a few issues show up in transportation and erection stages. To respond to such shortcomings, using pneumatic foam filled elements, an effective

* Corresponding author.
E-mail addresses: nematiuts@gmail.com (S. Nemati)

doi: 10.5267/j.esm.2019.12.002

rapidly assembled modular structure is presented that can be used for post-disaster management as a temporary road system. In this regard, two high-density Polyethylene plates with a thickness of 2 mm (Fig. 1) are used as the facings and semi-rigid Polyurethane foam is used as the core material with a thickness of 96 mm. Utilizing the HDPE facings, fabricated with roughly 1200 studs/m2, higher pull-out strength, better buckling execution and debonding behaviour between facings and foam-core are achieved.

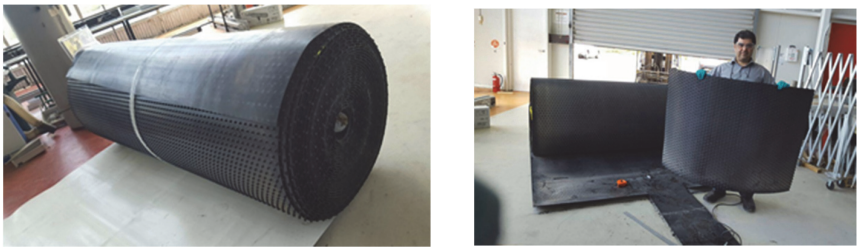

Fig. 1. 3-D high-density Polyethylene (HDPE) sheets

This system was created at the Centre for Infrastructure Engineering (CIE, Western Sydney University) for modular RABs and then a feasibility study on its application in post-disaster roads and sidewalks has been run in Central Queensland University. In this system, after inflating a fabric formwork, PUR foam is injected between the bottom and top HDPE layers. Therefore, an integrated volumetric pavement system is built (Fig. 2). In this study, numerical and experimental feasibility analyses are performed to investigate the structural performance of this system under design loading conditions.

Fig 2. Specimens of the investigated creative pavement system

2. Research History

Lowe (1997) registered a patent and explained some methods for producing a wall, roadway, road or floor of cementitious material. Also, Ferris (2002) patented an improved interlocking road block system. Lizarralde and Johnson (2008) studied on prefabrication for post -disaster reconstruction. They avoided high-tech industrialized operations and focused on small-scale local entrepreneurs. Foam made elements are well known because they are light and have excellent insulation properties. Therefore, some researchers worked on mechanical properties of lightweight and rapidly assembled materials such as foams. For example, Sabuwala et al. (2010) studied the flexible polyether polyurethane foams under scissors shear. Noble et al. studied the fatigue crack growth in rigid PU foam under conditions of constant load-amplitude cycling (Noble & Lilley 1981; Zheng et al., 2010). Toubia and his colleagues studied the effects of core joints in sandwich composites under in-plane static and fatigue loads (Toubia & Elmushyakhi 2017). Their research confirmed that despite the face sheets' primary in-plane load-carrying mechanisms, core junction substantially influences the axial fatigue life of the structure.

3. Material Properties

3.1. Fabric formwork

Some researchers have run a decision-making system to identify the best pneumatic formwork textile (Nemati et al., 2017). Tests illustrated that the usage of Barrateen, a high density polyethylene or polypropylene unbalance woven fabric coated by low density polyethylene is the optimized decision for fabric formwork in the created system (Fig. 3).

Fig. 3. Barrateen fabric sheet

3.2. Core material

3.2.1. Compressive behaviour

To identify the structural behaviour of the rigid Polyurethane foam some compressive tests have run based on the ASTM E1730 (ASTM 2015) (Fig. 4). The test results as well as the manufacturing properties are shown in Table 1.

Fig. 4. Loading test for determining the compressive properties of selected foam

Table 1. Structural and manufacturing specification of the studied foam

Structural specification			
Density: 192 kg/m^3	Compressive yield strength: 3.51 MPa	Tensile strength: 1.896 MPa	Shear strength: 1.034 MPa
Manufacturing specification			
Cream time: 35-40 sec	Free rise density: 280 – 300 kg/m^3	Tack free time: 115 ± 5 sec	Gel time: 94 ± 4 sec

3.2.2. Flatwise impact resistance

To examine the effect of transverse impacts such as brake effect of vehicles, a quasi-static impact test was used to simulate a low-velocity impact according to ASTM D2126. The face of each foam specimen (610 mm long, 610 mm wide and 50 mm thick) is bonded to a 0.8 mm thick aluminum sheet. For determining the impact resistance a 31.7 kg steel hemispherical cylinder of 80 mm diameter was dropped vertically from 762 mm distance so that the hemispherical end of the weight strikes the center of the

outer skin of the specimen on a horizontal plane. Investigation showed impact did not result in rupture to either skin or core foam. Also, no crushing of core is allowed outside a 76.2 mm radius from the centre of the impact (D2126 2015). The maximum crushing radius was measured as 21 mm. Therefore, the result shows an acceptable impact resistance for the specimens. Fig. 5 shows the crushing areas of skin and core foam, respectively.

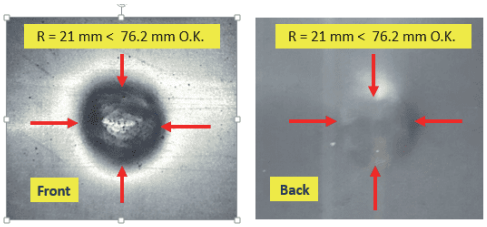

Fig. 5. The crushing areas of skin and core foam

3.3. High density polyethylene facings

To identify the tensile behaviour of the facings, longitudinal and transverse tensile tests were run on the HDPE plates following ASTM D5199 (Standard, 2012), ASTM D1505 (ASTM 2010) and ASTM D6693 (Testing and Materials 2004). Results illustrated that the module of elasticity in the lengthwise (EL) and crosswise (EC) directions are 131.33 MPa and 187 MPa, respectively. Therefore, to model the HDPE sheets as isotropic materials, the average value of module of elasticity (ESTUD = 159 MPa) was used (Sharafi et al. 2018a,b) (Table 2).

Table 2. Structural properties of the HDPE facings

Density (g/cm^3)	Tensile yielding strength (MPa)	Shear yielding strength (MPa)	Break elongation (%)	Stud pull-out strength (kN/m^2)	Average module of elasticity (MPa)
0.94	20.2	5.2	500	670	159

4. Composite Properties

4.1. Flatwise compressive behaviour

Four specimens were tested to determine the flatwise compressive behaviour and module of elasticity of the core material following the ASTM C365. Fig. 6 shows the results and stress-strain curves. Results showed that the average module of elasticity and yielding stress of the sandwich panels is 147.6 MPa and 4.3 MPa, respectively.

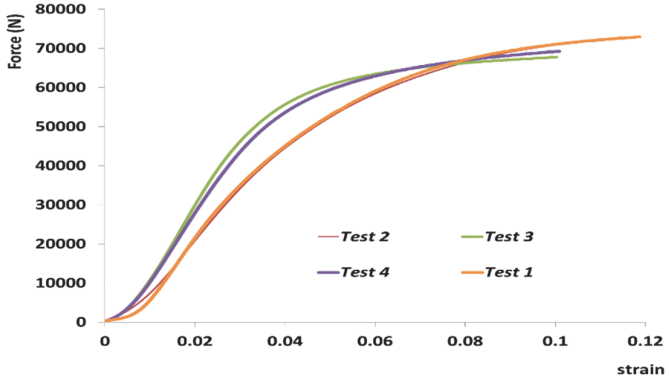

Fig. 6. Flatwise compression experiments results

4.2. Bending behaviour

4.2.1. Under uniform loads

In this test, the panels were loaded into the test rig, fixed and sealed before the suction is applied. The

loading rate can be changed according to the requirements. Fig. 7 shows the vacuum test rig setup and locations of automatic electrical potentiometers.

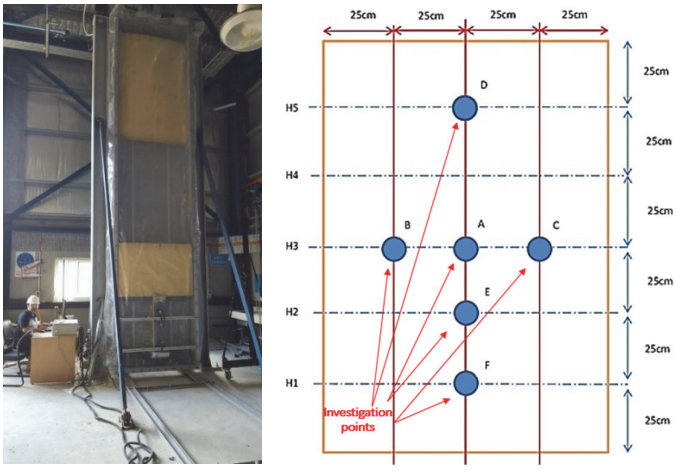

Fig. 7. The vacuum testing rig and arrangement of potentiometers on the specimens

Three monotonic tests were conducted on the specimens. All panels resisted a maximum of 0.77 atm. Up to a pressure of about 0.23 atm, where shows a large primary deflection, the system is in the adjusting phase, and the pressure is not directly resisted by the panels. Afterward, the PU foam panels exhibit a relative liner behaviour up to about 0.77 atm. In addition, the panel showed a symmetric curvature under the applied monotonic load (Fig. 8).

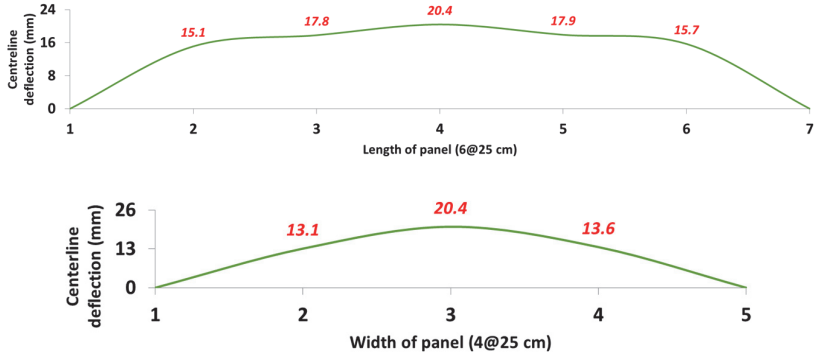

Fig. 8. The deflection pattern at longitudinal and transverse sections

4.2.2. Under concentrated loads

According to a series of experimental tests based on ASTM C393 and ASTM D7250, the core shear ultimate stress, facing bending stress and core shear modulus of introduced pavement system are determined as 1.9 MPa, 96.9 MPa and 11.3 MPa respectively (Fig. 9).

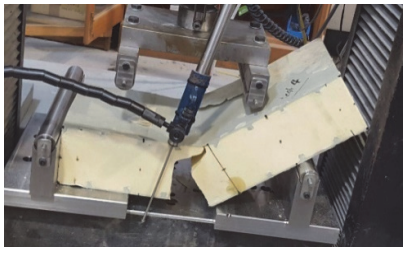

Fig. 9. Bending test of created system specimen

4.3. Ductility

Ductility plays a vital role in the design of pavement systems. Therefore, the torsional rigidity and rotational stiffness of the mentioned composite pavement system are investigated. In this regard, three L shape specimens are tested using a monotonic cantilever loading rig.

Fig. 10. Cantilever configuration of experimental tests

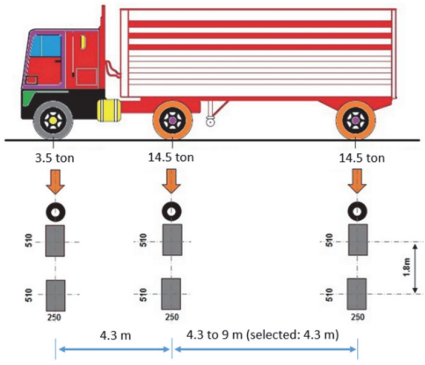

Fig. 11. AASHTO HL-93 truck loading configuration

The relative rotation of any two points can be calculated as the difference of related inclinometers rotations at each point. Using this test method, the torsional rigidity and rotational stiffness of the mentioned system are calculated as 93% and 14.5 kN.m/Rad, respectively. Other strength properties including fracture toughness and crack growth behaviour of foam materials are also important issues that are investigated extensively in previous works (e.g. Apostol et al., 2015; Aliha et al., 2018, 2019; Marsavina et al., 201,2015).

5. Pavement bearing and deformation control

In this step, a longitudinal element of composite pavement is modelled using finite element analysis commercial software of ANSYS. In this regard, AASHTO HL-93 truck (vehicular live load) is applied on the top surface of composite pavement (Fig. 11). Because the main application of the presented system is related to post-disaster management, a typical un-compacted soil including clay and sand is selected from literature as subgrade with a modulus of 0.00951 N/mm^3. As can be seen in Fig. 12, the maximum equivalent stress and the maximum shear stress are 1.46 MPa and 0.77 MPa, respectively, which are less than elastic limits of composite material.

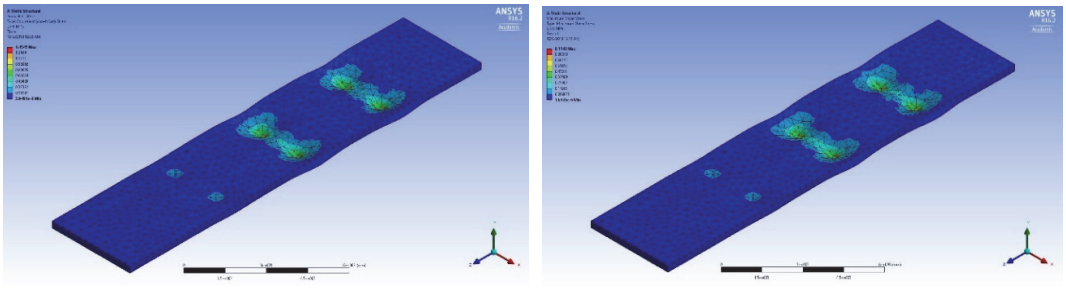

Fig. 12. Maximum equivalent stress (left) and maximum shear stress (right) in the pavement body

Also, the total deformation of the pavement under the AASHTO axles would be about 10.8 mm (Fig. 13). As mentioned above, the pavement remains in the elastic area under the AASHTO axles. Therefore, this deformation is temporary and will disappear after passing the live load. Other researchers have also performed similar finite element analyses for investigating the loading and deformation behaviour of pavements under traffic loading (Ameri et al., 2011; Aliha & Sarbijan, 2016; Loizos et al., 2009; Aliha et al., 2012; Nezhad & Fakhri, 2015; Fakhri et al., 2009)

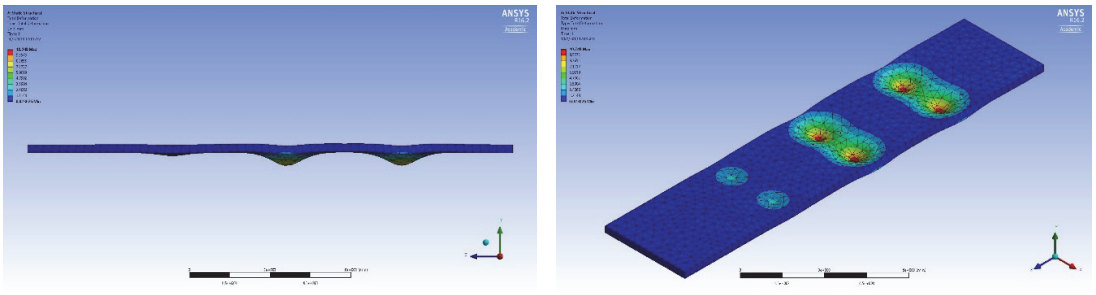

Fig. 13. Maximum elastic deformation of pavement system (scale 50x)

6. Conclusion

Based on the test results and numerical modelling the following conclusions are drawn:

- The maximum equivalent stress at the pavement body under the AASHTO loading truck is 0.77 MPa, which is less than the elastic limit of the composite system (4.3 MPa).
- The maximum shear stress at the pavement body under the AASHTO loading truck is 1.46 MPa, which is less than the ultimate shear stress of the composite system (1.9 MPa).
- Under monotonic loads, the created pavement has integrated and symmetric bending behaviour.
- The maximum deformation of the presented pavement system under temporary loading, even if it is supported to an uncompacted subgrade is in the elastic range and reversible.
- The rigidity and rotational stiffness of the mentioned temporary pavement system are about 93% and 14.5 kN.m/Rad, respectively. On the other hand, the created pavement system has acceptable impact resistance and damping behaviour under temporary traffic loads. Therefore, it has advantages of both rigid and flexible pavements at the same time.

References

ASTM (2010). Standard test method for density of plastics by the density-gradient technique.

ASTM (2015). ASTM-E1730, Standard Specification for Rigid Foam for Use in Structural Sandwich Panel Core, in ASTM International.

Aliha, M. R. M., & Sarbijan, M. J. (2016). Effects of loading, geometry and material properties on fracture parameters of a pavement containing top-down and bottom-up cracks. *Engineering Fracture Mechanics, 166*, 182-197.

Aliha, M. R. M., Ameri, M., Mansourian, A., & Ayatollahi, M. R. (2012). Finite element analysis of a new test specimen for investigating mixed mode cracks in asphalt overlays. *In 7th RILEM International Conference on Cracking in Pavements (pp. 359-367). Springer, Dordrecht*.

Aliha, M. R. M., Linul, E., Bahmani, A., & Marsavina, L. (2018). Experimental and theoretical fracture toughness investigation of PUR foams under mixed mode I+ III loading. *Polymer Testing, 67*, 75-83.

Aliha, M. R. M., Mousavi, S. S., Bahmani, A., Linul, E., & Marsavina, L. (2019). Crack initiation angles and propagation paths in polyurethane foams under mixed modes I/II and I/III loading. *Theoretical and Applied Fracture Mechanics, 101*, 152-161.

Ameri, M., Mansourian, A., Khavas, M. H., Aliha, M. R. M., & Ayatollahi, M. R. (2011). Cracked asphalt pavement under traffic loading–A 3D finite element analysis. *Engineering Fracture Mechanics, 78*(8), 1817-1826.

Apostol, D. A., Constantinescu, D. M., Marsavina, L., & Linul, E. (2015). Mixed-mode testing for an asymmetric four-point bending configuration of polyurethane foams. *In Applied Mechanics and Materials* (Vol. 760, pp. 239-244). Trans Tech Publications.

D2126, A. (2015). Standard Test Method for Response of Rigid Cellular Plastics to Thermal and Humid Aging.

Dandan, T. A. N., Wei, W. A. N. G., Jian, L. U., & Yang, B. I. A. N. (2007). Research on methods of assessing pedestrian level of service for sidewalk. *Journal of Transportation Systems Engineering and Information Technology, 7*(5), 74-79.

Development, U. S. D. o. H. a. U. (2014). ESG Minimum Habitability Standards for Emergency Shelters and Permanent Housing. USA.

Fakhri, M., Fakhri, M., & Kheiry, P. T. (2009). Modeling of top-down cracking (TDC) propagation in asphalt concrete pavements using fracture mechanics theory. *Adv Test Charact Bituminous Material*, 681-692.

Ferris, S. (2002). Interlocking sidewalk block system, Google Patents.

Goodyear, R. (2014). Housing in greater Christchurch after the earthquakes:Trends in housing from the Census of Population and Dwellings 1991–2013. New Zealand, Statistics New Zealand, Tatauranga Aotearoa.

Goodyear, R. K., & Fabian, A. (2014). *Housing in Auckland: Trends in housing from the Census of Population and Dwellings 1991 to 2013*. Statistics New Zealand.

Lizarralde, G., & Johnson, C. (2008). Myths and realities of prefabrication for post-disaster reconstruction. Building resilience achieving effective post-disaster reconstruction i-Rec.

Loizos, A., Partl, M. N., Scarpas, T., & Al-Qadi, I. L. (2009). Modeling of top-down cracking (TDC) propagation in asphalt concrete pavements using fracture mechanics theory. *In Advanced Testing and Characterization of Bituminous Materials, Two Volume Set* (pp. 713-724). CRC Press.

Lowe, M. (1997). Method for producing a wall, roadway, sidewalk or floor of cementitious material, Google Patents.

Marsavina, L., Constantinescu, D. M., Linul, E., Apostol, D. A., Voiconi, T., & Sadowski, T. (2014). Refinements on fracture toughness of PUR foams. *Engineering Fracture Mechanics, 129*, 54-66.

Marsavina, L., Constantinescu, D. M., Linul, E., Voiconi, T., & Apostol, D. A. (2015). Shear and mode II fracture of PUR foams. *Engineering Failure Analysis, 58*, 465-476.

Nezhad, S. R., & Fakhri, M. (2015). Studying the effect of vehicle speed on concrete pavement with finite element modeling (FEM). *International Conference on Research Science and Technology, Malaysia*.

Noble, F., & Lilley, J. (1981). Fatigue crack growth in polyurethane foam. *Journal of Materials Science, 16*(7), 1801-1808.

Sabuwala, T., Dai, X., & Gioia, G. (2010). Elastic Polyether Polyurethane Foams Under Punching: Experiments, Theory and Simulations. *ASME 2010 International Mechanical Engineering Congress and Exposition, American Society of Mechanical Engineers*.

Nemati, S., Rashidi, M., & Samali, B. (2017). Decision making on the optimised choice of pneumatic formwork textile for foam-filled structural composite panels. *International Journal of GEOMATE, 13*, 220-228.

Sharafi, P., Nemati, S., Samali, B., Bahmani, A., Khakpour, S., & Aliabadizadeh, Y. (2018). Flexural and shear performance of an innovative foam-filled sandwich panel with 3-D high density polyethylene skins. *Engineering Solid Mechanics*, *6*(2), 113-128.

Sharafi, P., Nemati, S., Samali, B., Mousavi, A., Khakpour, S., & Aliabadizadeh, Y. (2018). Edgewise and flatwise compressive behaviour of foam-filled sandwich panels with 3-D high density polyethylene skins. *Engineering Solid Mechanics*, *6*(3), 285-298.

Standard, A. (2012). Standard Test Method for Measuring the Nominal Thickness of Geosynthetics.

ASTM. (2010). Standard test method for determining tensile properties of nonreinforced polyethylene and nonreinforced flexible polypropylene geomembranes. *D6693-04*.

Toubia, E. A., & Elmushyakhi, A. (2017). Influence of core joints in sandwich composites under in-plane static and fatigue loads. *Materials & Design*, *131*, 102-111.

Tsai, M. K. (2014). Designing Postdisaster Temporary Housing Facilities: Case Study in Indonesia. *Natural Hazards Review*, *16*(3), 05014007.

Zheng, N., Liu, J., Wang, Q., & Liang, Z. (2010). Heavy metals exposure of children from stairway and sidewalk dust in the smelting district, northeast of China. *Atmospheric Environment*, *44*(27), 3239-3245.